

# DEVELOPMENT OF AN ALL-SKY ASSIMILATION OF MICROWAVE IMAGER AND SOUNDER RADIANCES FOR THE JAPAN METEOROLOGICAL AGENCY GLOBAL NUMERICAL WEATHER PREDICTION SYSTEM

Masahiro Kazumori and Takashi Kadowaki

Japan Meteorological Agency, 1-3-4 Otemachi, Chiyoda-ku, Tokyo, Japan

## Abstract

In numerical weather prediction (NWP), the assimilation of cloud- and precipitation- affected radiance is necessary to obtain accurate initial fields in cloudy areas. The cloud and precipitation phenomena exhibit nonlinear behaviors in their formation and dissipation. To consider such nonlinearity in an incremental four-dimensional variational (4D-Var) data assimilation, the outer-loop iteration is an effective method. In this method, the updates of the trajectory and the recomputations of the departures from the observations are performed in the minimizations of the 4D-Var data assimilation. Currently, cloud- and precipitation- affected radiance observations from polar-orbit satellites are not assimilated in the Japan Meteorological Agency (JMA) operational global NWP system. Moreover, in the 4D-Var data assimilation, the outer-loop iteration is not used to reduce the computational costs in the operational system. In this study, we examined the impacts of introducing the outer-loop iteration into the JMA global NWP system. During the minimization of the 4D-Var data assimilation, a single update of the trajectory and the recomputation of the departure from the observations are performed. The experimental results show that the introduction of the outer-loop iteration resulted in significant improvements in the tropospheric analysis and forecast accuracy, particularly in the temperature, humidity, and wind fields even when only the same observation dataset was used as the operational system. Then, on top of the introduced outer-loop system, microwave imager [Advanced Microwave Scanning Radiometer 2 (AMSR2), Global Precipitation Measurement (GPM) Microwave Imager (GMI) and Special Sensor Microwave Imager/Sounder (SSMIS)] and humidity sounder [Microwave Humidity Sounder (MHS) and GMI] radiance data were assimilated under the all-sky condition. The all-sky assimilation resulted in further improvements in the lower tropospheric temperature, water vapor, and wind fields in the analysis and forecast. Furthermore, increases in the used data counts of the water vapor-sensitive observations (e.g., clear-sky radiance data from geostationary satellites) in the system were confirmed. The major part of the improvements in the lower troposphere resulted from the all-sky assimilation of the microwave imagers, and the microwave humidity sounder contributed to the improvements in the middle and upper tropospheric humidity and wind fields.

## INTRODUCTION

Space-based microwave observations contain various information on geophysical parameters, e.g., atmospheric water vapour, cloud water, precipitation, surface wind and surface temperature over ocean. The information has been crucial for operational numerical weather prediction and climate research. However, present microwave radiance data assimilation focuses on atmospheric water vapour information because cloud and rain affected radiance data are not assimilated in the operational JMA global data assimilation system. The research objective is to obtain temperature and water vapor information in cloudy areas. Cloudy areas are sensitive to forecast accuracy of severe weather events (e.g., heavy precipitation, tropical cyclone, mid-latitude cyclone associated with convective storms). Improvements of analysis in the cloudy areas must bring better precipitation and tropical cyclone predictions. We reported our development status of the all-sky microwave radiance assimilation system for Japan Meteorological Agency (JMA) global numerical weather prediction system in Kazumori (2016). This paper describes latest updates on our development of the all-sky data assimilation system.

## METHODOLOGY

In this research, four components of all-sky microwave radiance assimilation are used. 1) Cloud and precipitation radiative transfer model. RTTOV-SCATT developed by NWP-SAF in EUMETSAT is used. 2) Cloud and precipitation-capable forecast model. JMA's operational global model, GSM (TL959L100) as of November 2016, is used. 3) Microwave radiance observations. Operationally available microwave imager radiance data, i.e., AMSR2, SSMIS and GMI, and microwave sounder radiance data, i.e., MHS and GMI are used. 4) 4D-Var data assimilation method is employed. In the JMA global 4D-Var data assimilation system, 6-hr assimilation window, and low-resolution tangent-linear and adjoint model are used in minimization of a cost function. No trajectory and FG (first-guess) departure (observation minus simulation) updates are performed during the minimization in the operational system.

An outer-loop iteration is introduced in the minimization of 4D-Var cost function which can help to include the non-linear process of cloud formation and precipitation. The outer-loop iteration updates trajectory and FG departures. Increase of QC-passed data is obtained from better FG fields.

Microwave imager radiance data, AMSR2, SSMIS, GMI (19, 23 and 37 GHz vertical polarized channels) are averaged with 4D-Var inner model's reduced gaussian grid (approximately 55 km horizontal resolution) and thinned with 150 km grid box in a pre-process of the data assimilation. Microwave sounder radiance data are thinned with 180 km grid box.

Observation error setting is one of the important parts in the all-sky radiance assimilation. Geer and Bauer (2011) proposed fundamental concept and their method are employed in this research. The all-sky observation error of microwave imager is defined based on a symmetric predictor  $C_{37}$ . This predictor is sensitive to cloud liquid water in 37 GHz observed and simulated radiances.  $C_{37}$  is defined an averaged cloud amount.

When the observation and the forecast model are unbiased each other as assumed in variational data assimilation, the statistics of FG departure should be symmetric. In Figure 1, the FG statistics are shown for AMSR2 19 GHz vertical polarized channel. A blue line in the left panel (a) which shows the FG departure's bias measured by the symmetric predictor. It is expected to be flat blue line when the mean cloud amount is used as the metric. The FG departure statistics shown in Figure 1 has a symmetric feature and it supports that all-sky microwave radiance data assimilation is applicable for the JMA global NWP system.

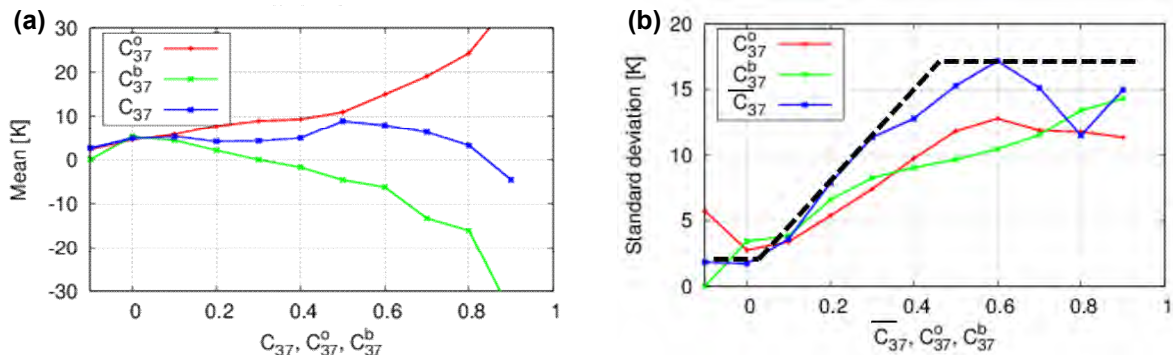


**Figure 1:** AMSR2 19 GHz vertical polarization channel's FG departure (a) bias and (b) standard deviation. Each line indicates dependency of cloud amounts shown in horizontal axis (Red: observed cloud amount, Green: background cloud amount and Blue: averaged cloud amount). Black broken line in panel (b) shows defined observation errors for use in the all-sky assimilation.

## DATA ASSIMILATION EXPERIMENT

Four data assimilation experiments were performed to investigate impacts of all-sky microwave imager and sounder radiance assimilation, and outer-loop introduction in the JMA global NWP system. Control run (CNTL) uses same configuration as JMA operational system as of November, in 2016. CNTL uses a clear sky microwave radiance assimilation configuration and no outer-loop iterations are used. TEST1 is an all-sky microwave imager and sounder radiance data assimilation with no outer-loop iterations. TEST2 is the same as CNTL but single outer-loop iteration (single update of the trajectory in the minimization and recomputations of FG departure for all observation type) is introduced. TEST3 includes the all-sky microwave radiance assimilation and the single outer-loop iteration.

In the TEST1 and TEST3 run, RTTOV\_SCATT is used for all-sky microwave radiative transfer calculation to include scattering and emission effects from hydrometeors in atmosphere. Temperature, water vapor, cloud liquid water, cloud ice water, cloud fraction, rain and snow profiles are obtained from JMA global model for the radiative transfer calculation. The symmetric observation errors defined with the symmetric cloud amount are used in the TEST1 and TEST3.

Figure 2 shows comparisons of assimilated microwave radiance observations (a) TEST1, (b) CNTL, and FG departures (c) TEST1, (d) CNTL for AMSR2. In the TEST1 run, increase of assimilated data and large FG departure in cloudy and rainy areas are confirmed. Dipole type FG departure distributions in the TEST1 (c) indicate information on the displacement of cloud and precipitation between observations and FG.

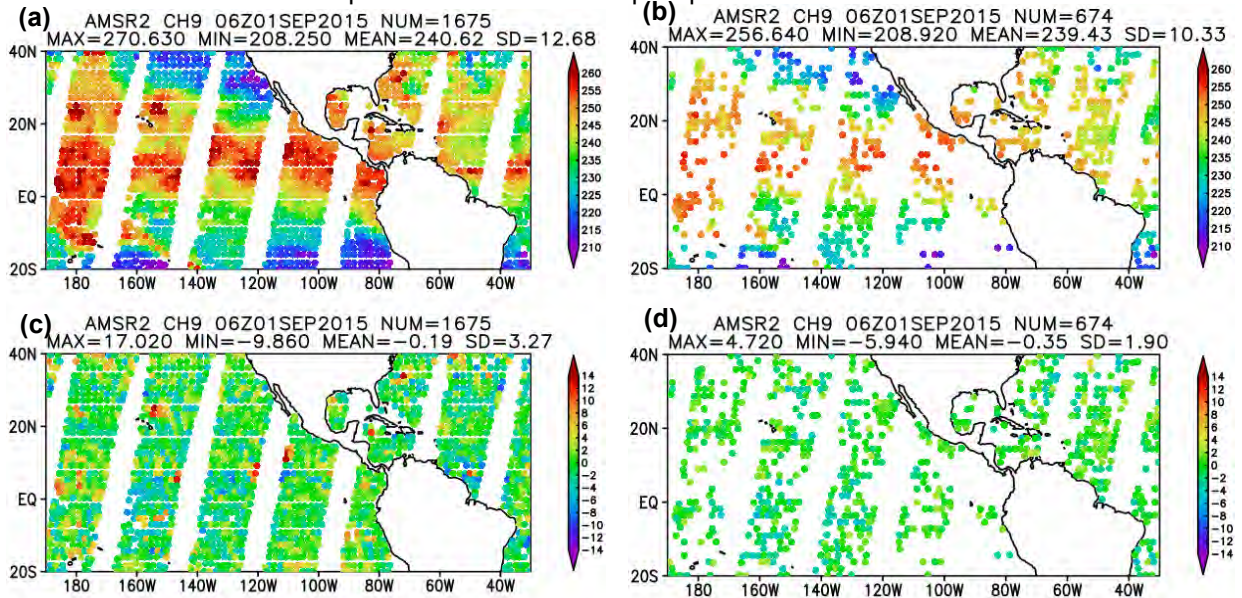


**Figure 2:** Comparisons of assimilated microwave radiance observations (a) TEST1, (b) CNTL, and their FG departures (c) TEST1, (d) CNTL of AMSR2 19 GHz V. The AMSR2 data are for 06 UTC 01 September 2015 analysis. The data statistics are shown at the top of each panel.

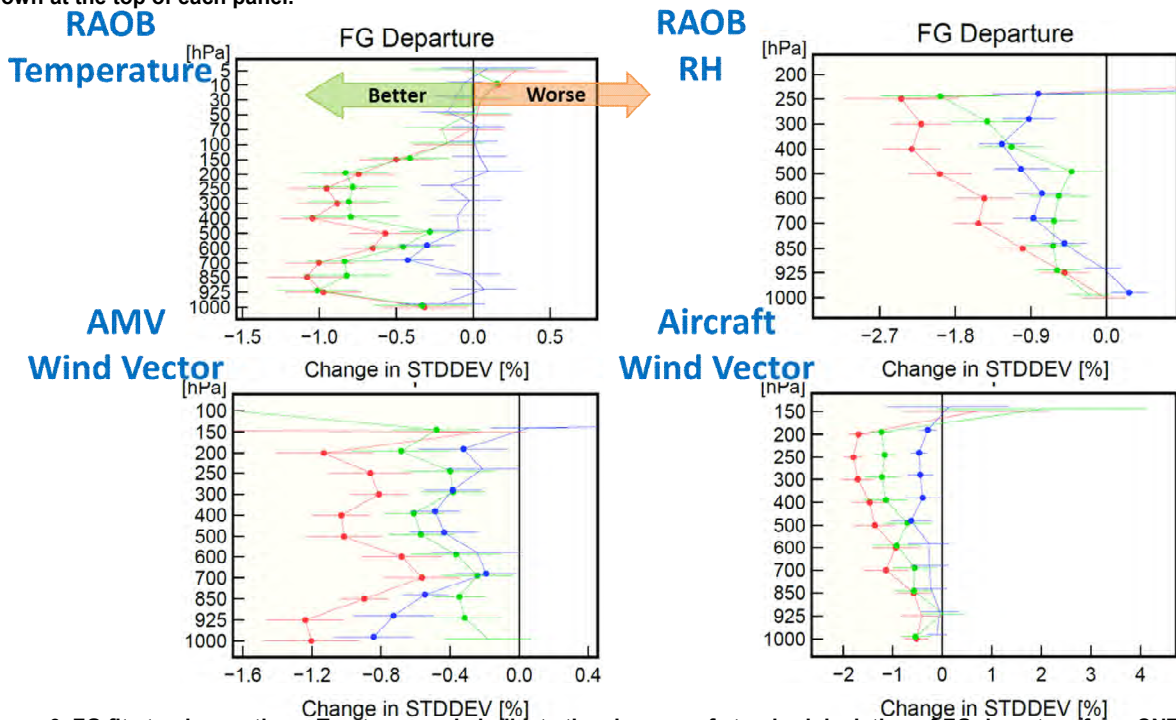


**Figure 3:** FG fits to observations. Top two panels indicate the changes of standard deviation of FG departure from CNTL run. Left panel is radiosonde temperature observation, right panel is radiosonde relative humidity observation. Bottom panels are same but for wind vector from atmospheric motion vector (AMV) (left) and aircraft data (right). Reductions of the standard deviation of FG departure indicate improvements of FG fields. Blue: TEST1, Green: TEST2, Red: TEST3. Filled circles indicate statistical significance.

FG fits to observations are shown in Figure 3. These are changes of standard deviation of FG departure from the CNTL run. Decreased values indicate improvements (i.e., reductions of forecast errors in the FG field). Top two panels indicate the change for radiosonde observations, temperature (left) and relative humidity (right). Bottom two panels indicate the changes for wind vector of atmospheric motion vector (AMV) (left) and aircraft data (right). Blue lines indicate the results from TEST1, green lines indicate the results from TEST2, and red lines indicate the results from TEST3. Generally, TEST cases showed improvements. Especially, the improvements of lower level wind and upper level humidity are obtained from all-sky assimilation of microwave imager and sounder radiance data, respectively. TEST3 results showed the best improvement among the experiments.

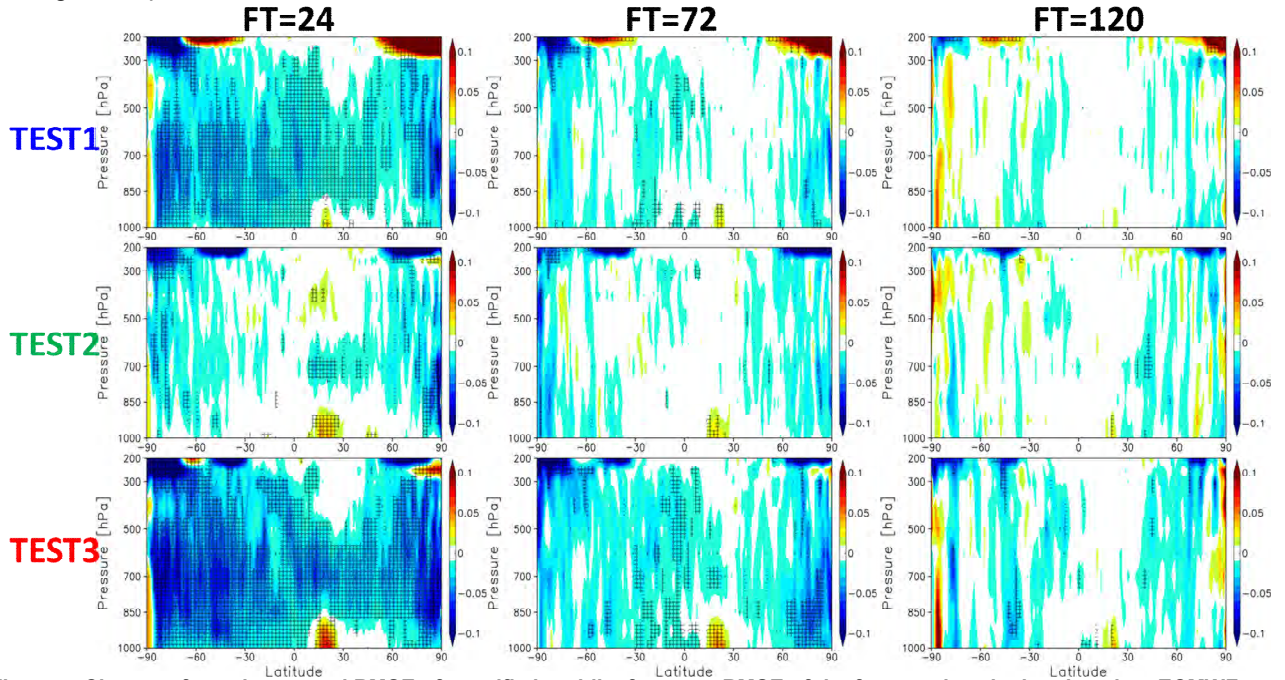


**Figure 5:** Change of zonal averaged RMSE of specific humidity forecast. RMSE of the forecast is calculated against ECMWF analysis. Left panel is 24-hr forecast, middle panel is 48-hr forecast, and right panel is 72-hr forecast. Top three panels are for TEST1, middle panels are TEST2 and bottom panels are TEST3. Blue colour indicates reductions of RMSE in TEST runs. Hatched areas indicate the changes are statistically significant.

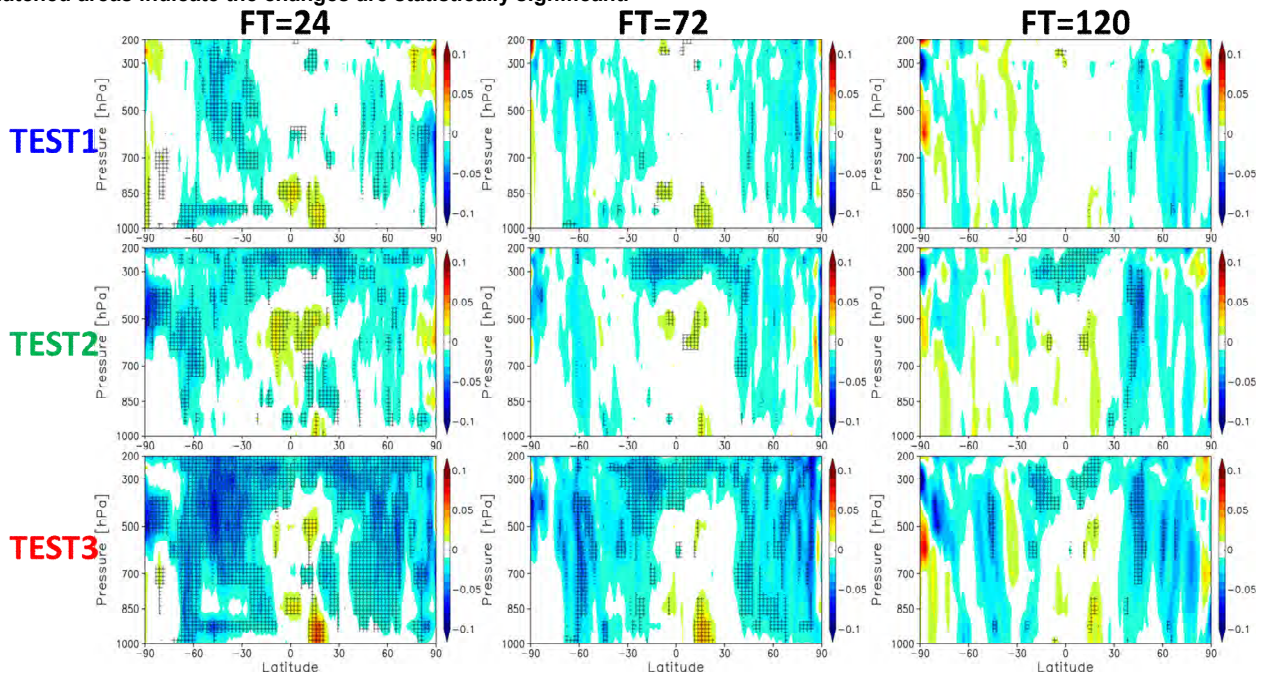


**Figure 6:** Same as Figure 5, but for temperature.

The forecast fields are verified against ECMWF analysis field. The change of zonal averaged RMSE of specific humidity forecast (Figure 5), temperature (Figure 6) and wind vector (Figure 7) are shown for TEST1, TEST2 and TEST3. The all-sky assimilation brought improvements of the short-range forecast of the tropospheric water vapor fields, globally. The outer-loop introduction (TEST2) indicated small improvements of the middle tropospheric water vapor field for the tropics. TEST3 results indicate significant improvement of water vapor fields globally. The improvements in the tropics and the northern hemisphere retained until 72-hour forecast. As for temperature fields (Figure 6), improvement in the mid-latitude troposphere were significant and TEST3 showed the largest improvement. Some degradations of the lower troposphere in the tropics were commonly confirmed for specific humidity and temperature fields.

In all-sky microwave radiance assimilation with ECMWF 4D-Var system, improvement of dynamical field (e.g. wind field) in the analysis and forecast are reported (Geer et al. 2017, Kazumori et al. 2016). In this research, similar improvements were confirmed in wind forecast verifications as shown in Figure 7. Generally, all-sky radiance assimilation with 4D-Var system could provide wind information from clouds and precipitation information tracking through the forecast model physics. The introduction of the outer-loop iteration enhanced the impact of the all-sky assimilation.

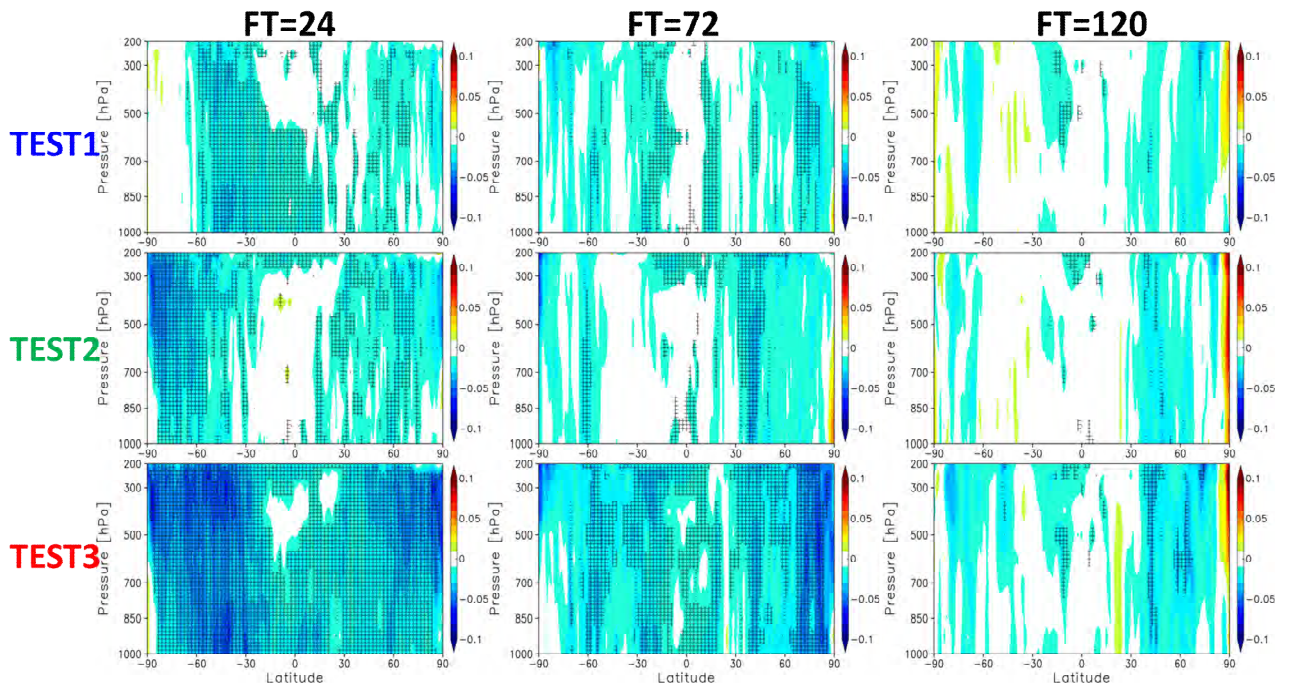


**Figure 7:** Same as Figure 5, but for wind vector.

Tropical Cyclone (TC) is one of the severe meteorological phenomena and its accurate prediction is important and challenging. Water vapor, clouds and precipitation have important roles for TC formation and development. Comparisons between TEST3 and CNTL for various TC cases showed clear positive impacts from the all-sky assimilation and the outer-loop introduction. Figure 8 shows the comparisons of the forecast errors of TC track predictions. The all-sky assimilation and the outer-loop introduction reduced the error of TC track predictions for various ocean basins. The results are consistent with the improvement of short-range forecast of temperature, specific humidity, and wind vector fields (shown in Figure 5, 6, and 7). Figure 9 shows one typical improved TC central pressure predictions (Hurricane Jimena 2015) from the data assimilation experiments. As shown in the left panels in Figure 9, TEST3 case (all-sky assimilation plus outer-loop introduction) showed a realistic rapid intensification of the TC compared to those of CNTL runs. The results from TEST2 showed improvements for the TC intensity predictions. However, TEST3 showed much realistic predictions of the rapid intensification (NOAA best track data are shown with a black line). The improvements were found in the development stages of the TC because the clouds were widely scattered around the centre of the TC and the areas were covered with clouds. The all-sky assimilation could increase the assimilated microwave radiance data for those areas. Much observational information on water vapor, clouds, and precipitation were assimilated in TEST3. However, minor improvements were found in the decaying stages for all cases.

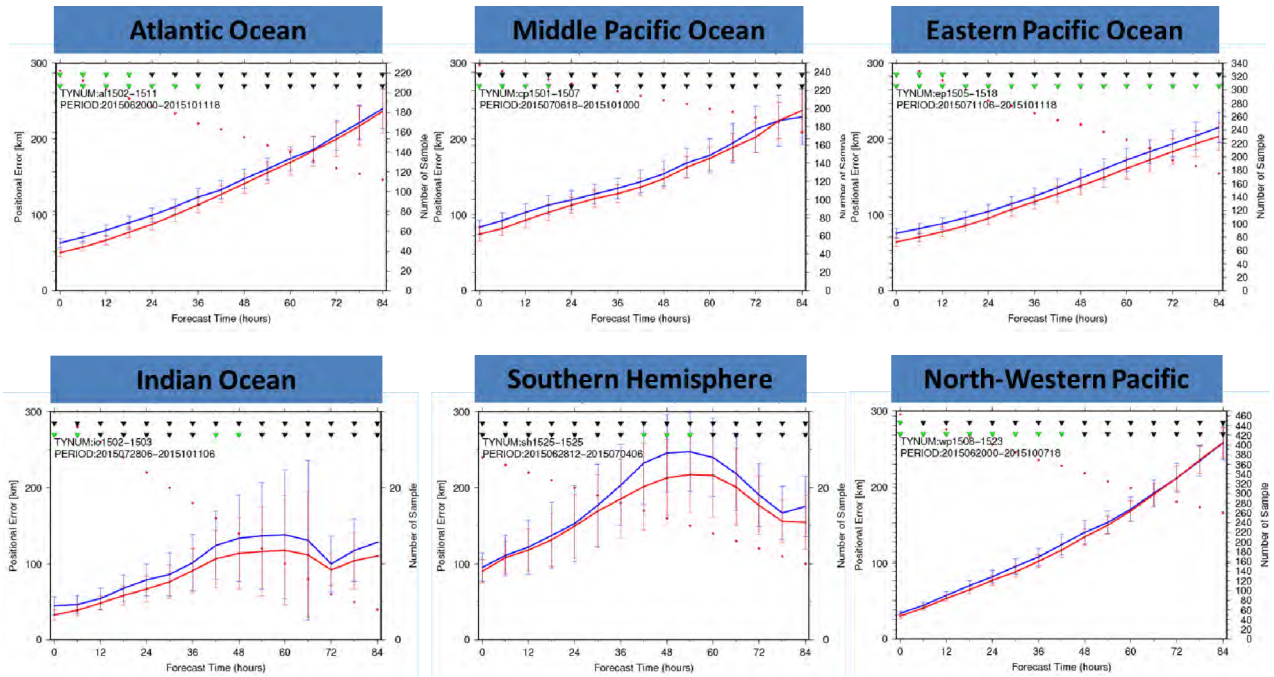


**Figure 8:** Comparison of forecast errors of TC track predictions between TEST3 (red) and CNTL (blue) for various ocean basins. Red points indicate number of samples with right axis for each panel. Triangle mark indicate statistical significance with green symbols. Upper triangle mark indicate statistical test results with temporal correlation and lower triangle mark indicate the same statistical results but without temporal correlation.

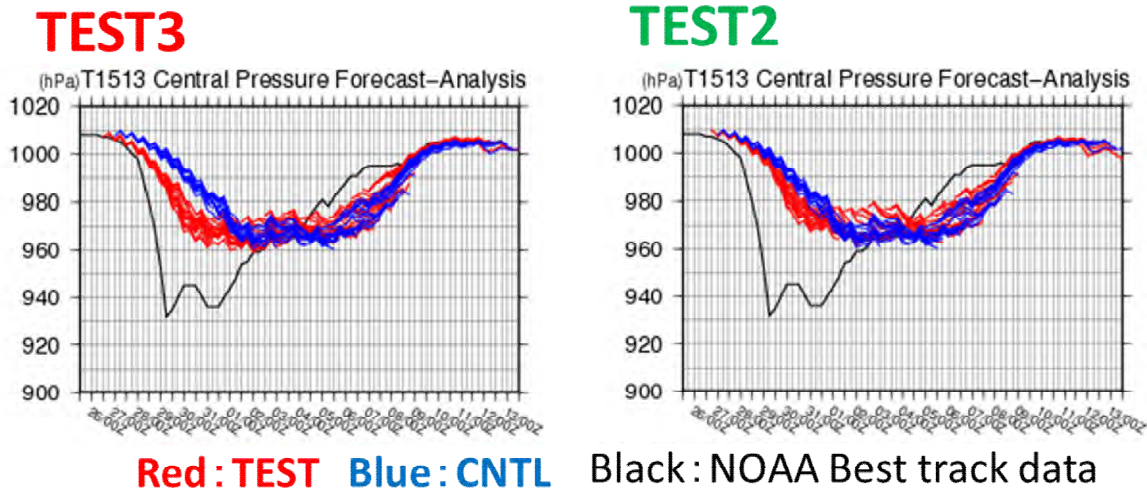


**Figure 9:** Comparison of central pressure prediction of a tropical cyclone (Hurricane Jimena 2015). Red lines indicate predicted central pressure from TEST runs (left: TEST3, right: TEST2). Blue lines indicate predicted central pressure from CNTL. Black lines indicate NOAA best track data.

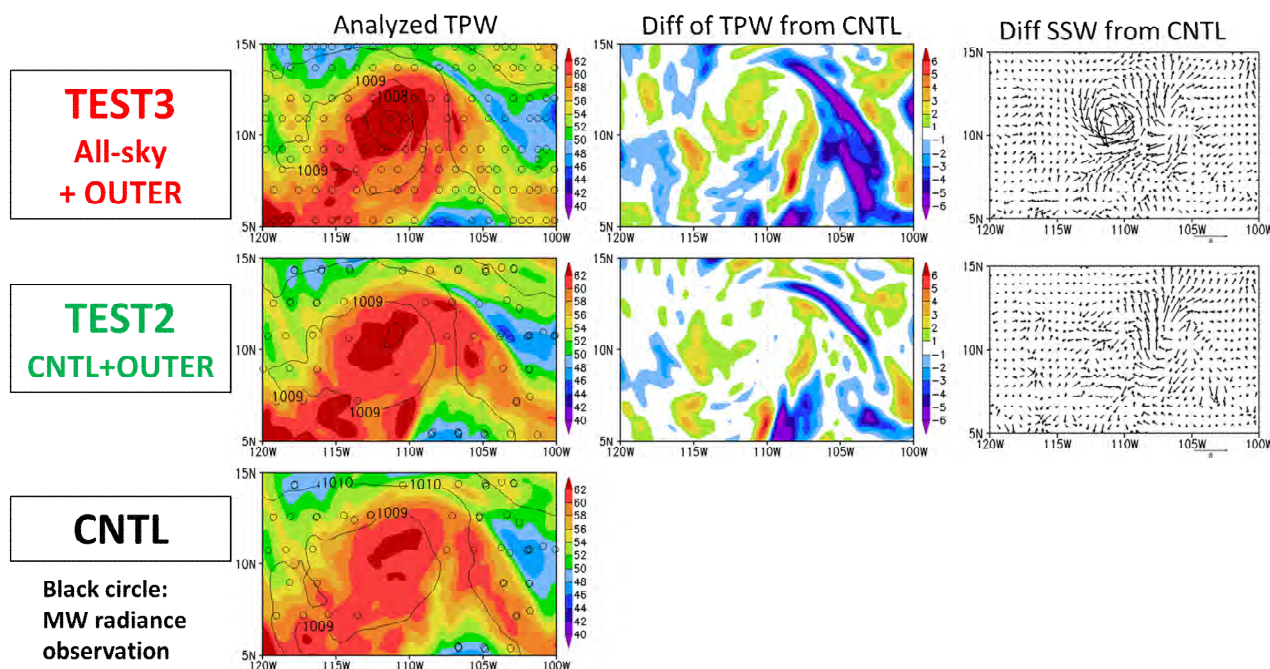


Figure 10: Comparison of analysed total precipitable water (TPW) vapor field and surface pressure fields (left panels) and TPW differences from that of CNTL (middle panels). Right two panels are vector differences of sea surface wind between TEST and CNTL. Top panels are TEST3, middle panels are TEST2 and bottom panel is CNTL. Black circles on the left panels indicate the location of assimilated microwave radiance data in the experiment.

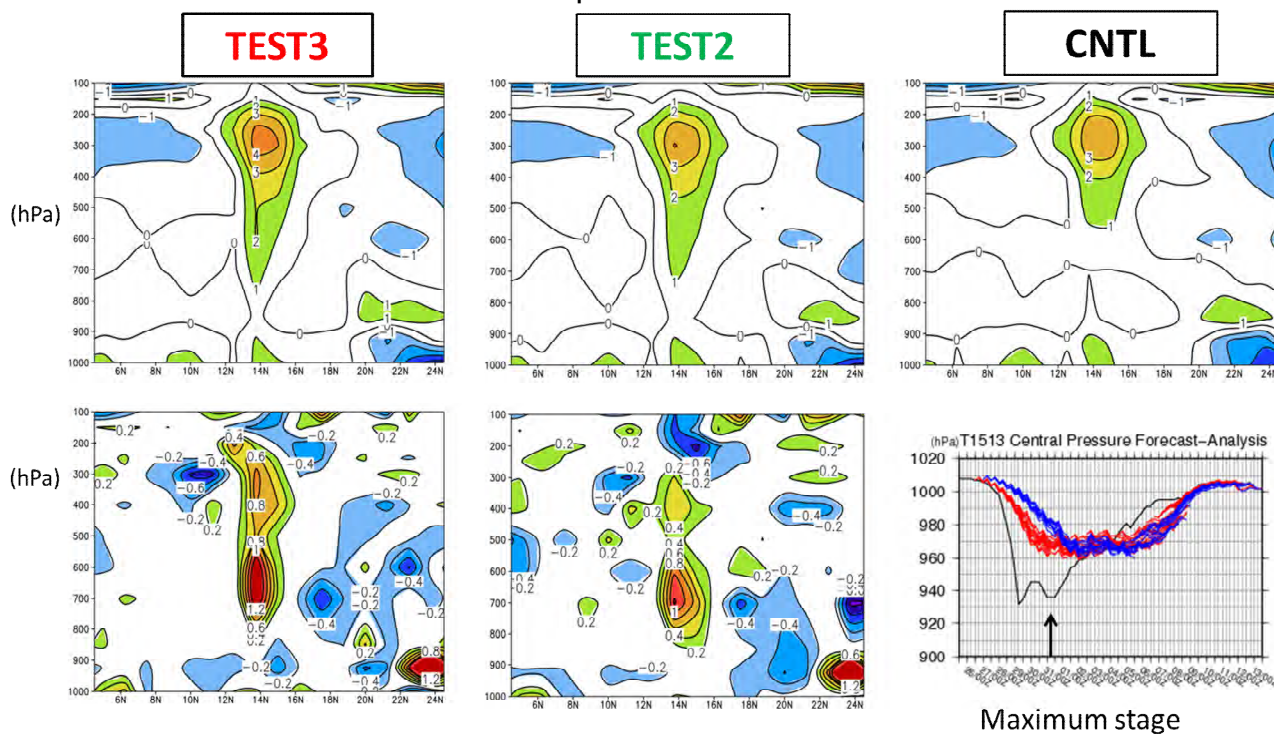


Figure 11: Temperature anomaly at the north-south vertical cross section in the centre of the TC at the maximum stage (shown in the right bottom panel). Bottom left, and middle panels are the difference from the TEST and CNTL. The units of the temperature anomaly.

To clarify the mechanism of the improved TC prediction by the all-sky radiance assimilation, water vapor fields in cloudy regions around the TC were compared. Figure 10 shows the comparison of total precipitable water (TPW) vapor analysis and their differences from CNTL run. Difference of analysed sea surface wind vectors are shown with arrows in the right panels. TEST3 result showed high TPW amount in the centre of

the TC was analysed in the all-sky assimilation and the outer-loop introduction. Black open circles indicate assimilated microwave radiance data. TEST2 result showed increased TPW around the TC centre through the clear sky assimilation and outer-loop introduction. The TEST3 results showed the all-sky assimilation plus the outer-loop introduction could change the water vapor and wind fields realistically under cloudy conditions (i.e., in the core of TC). Figure 11 shows comparisons of temperature anomaly at the vertical cross section (north-south direction) of TC centre at the maximum stage of the TC. TEST3 results showed the warmest core (approximately four Kelvin) in the upper tropospheric temperature fields.

Generally, in the TC genesis stage and developing stage, scattered cumulus clouds are widely spread, and they are in a circulation. In these stages, all-sky microwave radiance data assimilation can provide water vapor information under the cloudy situation and their assimilation result in increases of water vapor concentration in and around the TC centre. They help the enhancement of the circulation in the lower troposphere. The increase of water vapor, deeper central pressure and enhanced water vapor flows toward TC centre can be retained in the data assimilation cycle. In decaying stages, the impact of all-sky radiance assimilation was relatively small compared to the early stage of the TC lifetime. One possible explanation is that the amount of the clouds was decreased around the TC and there is an intrusion of relatively dry atmosphere from high latitude areas. The atmosphere is under clear conditions and clear-sky microwave radiance data have already assimilated in CNTL run.

The experiment results showed the all-sky assimilation can make realistic concentration of water vapour under cloudy conditions and they contribute to improved TC analysis and predictions. Moreover, enhanced warm core, strong surface wind in the vortex and a rapid intensification of tropical cyclones were successfully analysed and they contributed improved TC predictions.

## MODEL BIAS ISSUES

In the variational data assimilation, un-bias is assumed in both forecast model and observations. Careful investigations on microwave radiance's FG departure statistics revealed that JMA global model has biases relating to cloud representation. Figure 12 shows comparisons of SAPHIR 183 GHz brightness temperature between observation and simulation for the tropical area in 14 August 2016. SAPHIR's all-sky FG radiance data do not show realistic contract of the convective clouds. The results imply lower cloud top height in the atmospheric profiles obtained from the JMA global model.

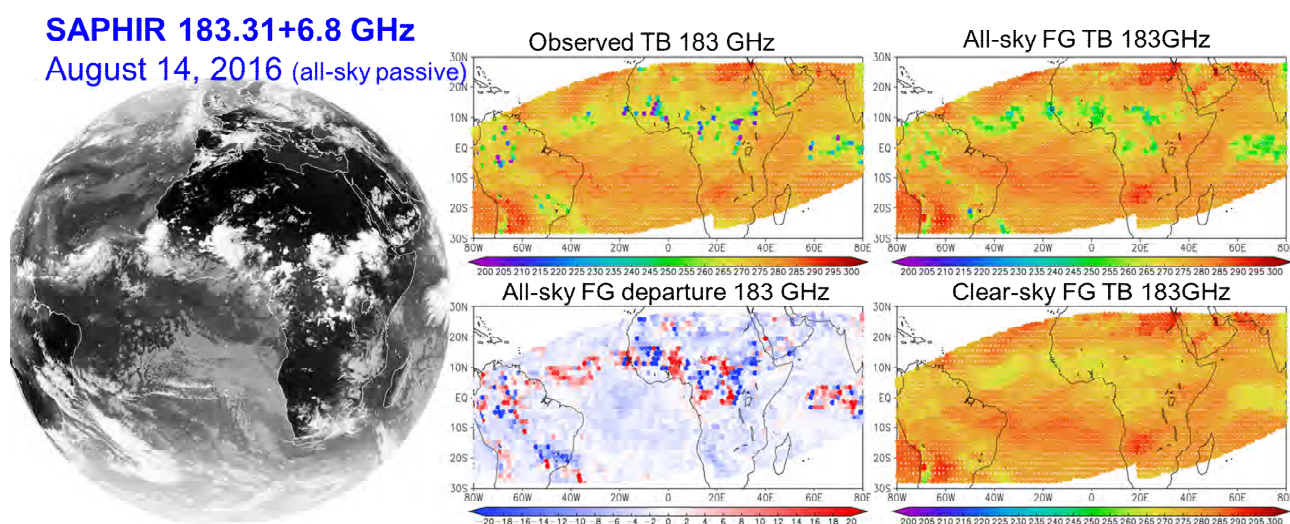


**Figure 12:** Right for panels: Distribution of observed brightness temperature, all-sky FG brightness temperature, all-sky FG departure, and clear-sky FG brightness temperature of SAPHIR 183.31+6.8 GHz in August 14, 2016. Left image is Meteosat-10 Infra-red image.

## SUMMARY

In this research, an all-sky microwave radiance assimilation system was developed for JMA's global 4D-Var data assimilation system. The all-sky assimilation can be expected to bring significant improvement of forecast in the JMA NWP system by the improvements of initial field under cloudy conditions. To investigate the impact of the all-sky radiance assimilation, data assimilation experiments of all-sky microwave radiance

were performed. Furthermore, to include non-linearity of cloud formation and dissipation in the analysis, an outer-loop iteration was introduced and its impact was examined separately. From the assimilation experiments, improved analysis and FG fields of water vapour, temperature, wind in the troposphere, especially cloudy and rainy conditions were found. Remarkable impacts of the all-sky radiance assimilation were improvements of TC analysis and predictions. These are valuable results from a point of view as operational NWP system, because generally, TC prediction is one of the most important information for reduction of social and economic damage from natural hazard although generally it is difficult to produce their accurate predictions. In the genesis and developing stages of TC, increase of TPW and TPW concentration under cloudy conditions were analysed from the all-sky radiance assimilation. Furthermore, much realistic rapid intensifications through the data assimilation cycle were represented in the all-sky radiance assimilation. These improvements of TC intensity analysis and prediction are thought as direct benefits from all-sky radiance assimilation. Because assimilated data were increased in the cloudy areas where the data had not been assimilated. In steady and decaying stages of TC, impacts were not large. One plausible reason of the small impacts is that transition from TC to extra-tropical cyclone is dominated by large-scale synoptic feature. However, improvement in mid-latitude atmospheric circulation (representation of trough and ridge) by the all-sky microwave radiance assimilation could bring better TC track prediction in medium range forecast. The improvement of TC track prediction is thought as indirect benefits of the all-sky assimilation.

All-sky FG departure of SAPHIR radiance revealed the JMA global model's biases in convective clouds. They suggest model's cloud top height is underestimated. This kind of comparisons between the observation and the simulation provide useful information for NWP model developments. The all-sky radiance assimilation relies on accuracy of FG clouds and precipitation. Forecast model biases in cloud physics and convective scheme would cause spurious increment in the analysis. To obtain temperature and humidity information from the observation and make consistent changes among physical variables (i.e., temperature, humidity, clouds, and rain), reductions of these forecast model biases are inevitable.

## REFERENCES

Geer, A. and P. Bauer, (2011) Observation errors in all-sky data assimilation. *Quarterly Journal of the Royal Meteorological Society*, **137**, pp 2024-2037.

Geer, A. J., F. Baordo, N. Bormann, P. Chambon, S. J. English, M. Kazumori, H. Lawrence, P. Lean, K. Lonitz and C. Lupu, (2017) The growing impact of satellite observations sensitive to humidity, cloud and precipitation. *Quarterly Journal of the Royal Meteorological Society*, **143**, 3189-3206.

Kazumori, M., A. J. Geer and S. J. English, (2016) Effects of all-sky assimilation of GCOM-W/AMSR2 radiances in the ECMWF numerical weather prediction system, *Quarterly Journal of the Royal Meteorological Society*, **142**, pp 721-737

Kazumori, M., (2016) Development of all-sky microwave radiance assimilation for JMA global NWP system. *Proceedings for the 2016 EUMETSAT Meteorological Satellite Conference*, 26-30 September 2016, Darmstadt, Germany.